

RAPID SOLIDIFIED MG-CA-ZN ALLOYS WITH MICROALLOYING OF LA, ND, Y, ZR

Tatiana V. Larionova*, Bong-Sun You**

***St.Petersburg State Polytechnical University, **Korea Institute of Materials Science**

Keywords: *Magnesium alloys; rapid-solidification; mechanical properties; age hardening*

Abstract

Mg-Ca-Zn-X alloys (with Ca content from 0.89 to 3.19 at.%, Zn from 1.2 to 4.23 at.% and X = La, Nd, Y, Zr) were prepared by a melt spinning and studied by XRD, micro-hardness test and microstructure observation. Depending on the composition, the alloys solidified as: a single phase - Mg solid solution; a two phase mixture - Mg-based solid solution and Mg₂Ca or Mg₆Ca₂Zn₃; or a three phase mixture - Mg solid solution, Mg₂Ca and Mg₆Ca₂Zn₃. As-solidified ribbons exhibited hardening according to the following: $HV = 50 + 18C_{Ca} + 8 C_{Zn}$, where C_{Ca} and C_{Zn} are Ca and Zn content correspondingly. The higher Ca impact is explained by its stronger refinement effect. Several age-hardening phenomena were observed. The most significant effect was revealed in Mg-2.99at.%Ca-2.32at.%Zn.

Key words: *Magnesium alloys; rapid-solidification; X-ray diffraction; mechanical properties*

1 . Introduction

The rapid solidification technique is believed to be able to eliminate such Mg-based alloys limitations as low strength, restricted plasticity at an ambient temperature and poor corrosion resistance [1-3]. The refinement of the matrix and the size and spacing of the precipitates occurred under rapid crystallization gives essential improvement to most of the mechanical properties [2]. Except this, the rapid solidification provides a formation of supersaturated solid solution, further decomposition of which may induce a significant precipitation hardening effect [1-4]. The present study is devoted to rapid solidified Mg-Ca-Zn alloys with additions of Y, Nd, Zr, La. Calcium is known as to provide creep and corrosion resistance, reduce the flammability of molten magnesium based alloys [5,6]. The solid solution of such elements as REM, Ca, Ni in magnesium results in substantial reduction of Mg lattice axial ratio (c/a) with the associated

enhancement of deformability [1,7]. As was mentioned grain refinement makes a significant contribution to improving the strength of Mg alloys as reported in, extrusion at high temperatures induces dynamic recrystallization and grain growth, so grain boundaries must be pinned with secondary-phase particles to inhibit grain growth [8]. Rapid solidification technique allows to extend the solid solubility Ca in Mg up-to about 2.0 at.% as reported in [9-10] over equilibrium maximum (0.82 at.%), what intensifies precipitation hardening through the formation of the Mg₂Ca phase. Having high decomposition temperature the Mg₂Ca was assumed to be a reason for the heat resistant of the Mg-Al-Ca alloys [5]. As reported in [11] the precipitation hardening of Mg-Ca alloys may be significantly enlarged with the addition of Zn, what was attributed to the formation of ternary metastable phases. A Zn addition to Mg-Ca alloy was found to result in the best combination of strength and ductility among others alloying elements [9].

Rare earth elements or yttrium weaken the strong basal textures and improve magnesium alloys formability [7]. Besides microalloying can influence precipitation hardening by refining the existing precipitate structure [8], or by promoting the formation of new precipitates [5,11]. The goal of the present work was to enhance strength and heat resistance of Mg-Ca-Zn-based alloys by microalloying and exploiting rapid solidification technique. In the present work Mg-Ca-Zn alloys prepared by rapid solidification and micro-alloyed with La, Y, Nd, Zr were studied in order to investigate the effects of alloying additions in conditions of non-equilibrium solidification on the mechanical properties, precipitation hardening and thermal resistance.

2. Materials and Methods

Mg-Ca-Zn alloys were melted from elements of 99.9 % purity by induction melting under a SF₆+CO₂ mixed gas atmosphere in a steel crucible. Ribbons of approximately 40 μm thick and 3-5 mm wide were prepared by melt-spinning under argon on a copper wheel. The designation and verified chemical composition of the alloys are listed in Table 1. Alloys designation and analyzed chemical composition (at.%)

Table 1.
Alloys designation and analyzed chemical composition (at.%)

Alloy	Mg	Ca	Zn	La	Nd	Y	Zr
MZC1	bal.	1.25	0.89	-	-	-	-
MZC2	bal.	2.30	0.83	-	-	-	-
MZC3	bal.	4.25	0.99	-	-	-	-
MZC4	bal.	1.25	2.97	-	-	-	-
MZC5	bal.	2.32	2.99	-	-	-	-
MZC6	bal.	4.23	3.19	-	-	-	-
MZCL	bal.	2.72	2.28	0,32	-	-	-
MZCN	bal.	2,60	2,09	-	0,19	-	-

MZCY	bal.	2,45	2,13	-	-	0,25	-
MZCZ	bal.	2,71	1,91	-	-	-	0,24

Isochronal and isothermal heat treatment was performed at temperatures ranging from 100 to 400°C. The specimens were wrapped in aluminum foil and heat treated in argon in a resistance furnace and then cooled on air. Phase analysis and lattice parameter determination were carried out by XRD method using CuK_α radiation, the ribbon's side contacting with the cooling wheel was examined. Lattice parameters were calculated according to center of gravity of the (1000) and (0002) peaks. For a microhardness test the ribbons were cold mounted on an edge and then polished. The test was fulfilled using a Vickers indenter with 10g load applied for 10 seconds. At least 10 measurements per each point were made. Foils for the TEM examination were prepared by an ion beam thinning technique.

3. Experimental results and discussion

Fig. 1(a-d) shows the XRD spectrum of the as-solidified ribbons. The alloys, depending on their compositions, solidified as: (i) a single-phase – Mg supersaturated solid solution (Mg_{ss}); (ii) a two-phase mixture - Mg_{ss} and Mg₂Ca [9,10,12] or a ternary phase identified as Mg₆Ca₂Zn₃ [13]; or (iii) a three-phase mixture - Mg_{ss}, Mg₂Ca and Mg₆Ca₂Zn₃. However, it should be noted that the ternary phase has a wide homogeneity field what was mentioned in [13] and discussed in detail in [14,15]. No phases containing La, Y, Nd were detected, even though after 1 hour 20' exposure at 400°C. The phases, identified by the XRD in as-solidified and annealed conditions are listed in Table 2.

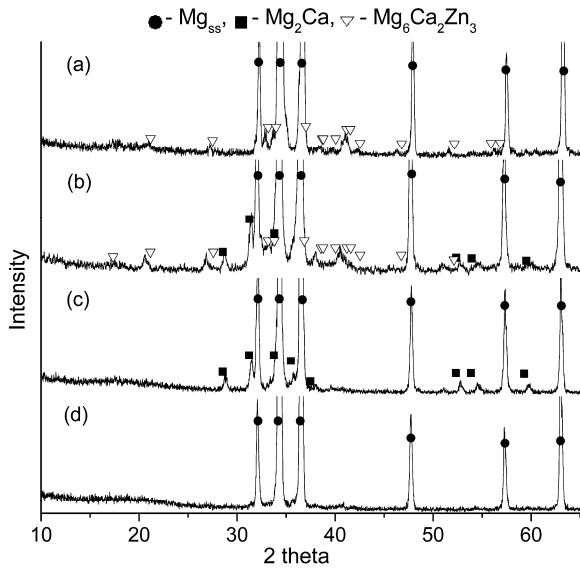


Fig.1. XRD data of as-solidified sample a) – MZC2, b) - MZC5, c) - MZC4, d) – MZC1.

Fig. 2(a) shows the microstructure of the MZC2 containing the ternary phase (Table 2). The sample exhibited dendritic structure with spherical precipitates with size of about 200 nm within the grains. The three-phase structure presented in MZC5 (Fig. 2(b)) has precipitates located within the grain and eutectic along the grain boundaries. The average grain size decreased with the increase of the alloying contents.

Table 2
Phases identified by XRD

Alloy	as-solidified	annealed at T = 400 °C, t = 1h
MZC1	Mg _{ss}	Mg _{ss} , Mg ₆ Ca ₂ Zn ₃
MZC2	Mg _{ss} , Mg ₆ Ca ₂ Zn ₃	Mg _{ss} , Mg ₆ Ca ₂ Zn ₃
MZC3	Mg _{ss} , Mg ₆ Ca ₂ Zn ₃ ,	Mg _{ss} , Mg ₆ Ca ₂ Zn ₃
MZC4	Mg _{ss} , Mg ₂ Ca	Mg _{ss} , Mg ₂ Ca, Mg ₆ Ca ₂ Zn ₃
MZC5	Mg _{ss} , Mg ₂ Ca, Mg ₆ Ca ₂ Zn ₃	Mg _{ss} , Mg ₂ Ca, Mg ₆ Ca ₂ Zn ₃
MZC6	Mg _{ss} , Mg ₂ Ca, Mg ₆ Ca ₂ Zn ₃	Mg _{ss} , Mg ₂ Ca (trace), Mg ₆ Ca ₂ Zn ₃

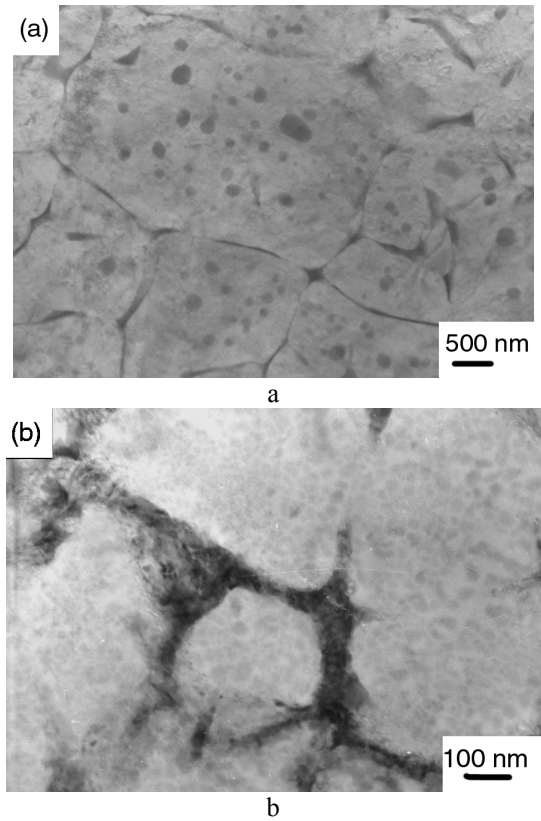


Fig. 2. Microstructure of as-solidified samples MZC2 (a), MZC5 (b).

In Fig. 3 the microhardness of the as-solidified ribbons is plotted versus the total alloying content, the experimental data are compared to the literature data for binary Mg-Ca [9,12,16] and Mg-Zn [3,17,19] rapidly solidified alloys.

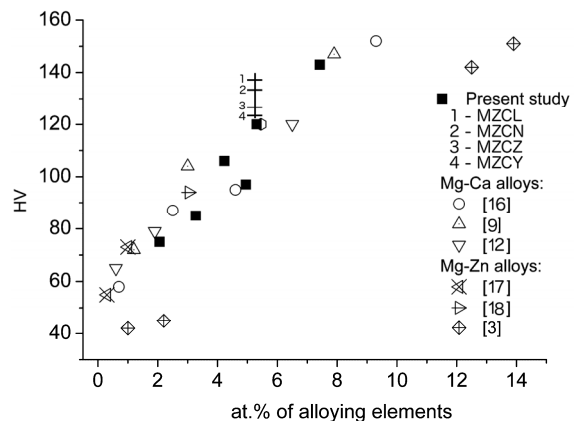


Fig. 3. Microhardness of rapidly solidified Mg-Ca-Zn alloys vs. total (Ca+Zn) alloying content compared with rapidly solidified binary Mg-Ca and Mg-Zn alloys.

The data for studied alloys are approximated well by a dependence: $HV = 50 + 18 C_{Ca} + 8 C_{Zn}$, where C_{Ca} and C_{Zn} are Ca and Zn content correspondently. Thus,

18kg/mm²at.% and 8kg/mm²at.% are the hardening effects induced by Ca and Zn correspondently. Excellent correlation of the data with Hall-Petch equation, presented in Fig. 4, justifies that as-solidified alloy's microhardness is mainly determined by the microstructural refinement. The Hall-Petch coefficient was found to be 0.18 MPam^{-1/2}, what is less than that for Mg with coarser grain structure (0.7 MPa m^{-1/2}) [8]. The higher Ca strengthening impact is explained by its stronger refinement effect over Zn. All quaternary micro-alloyed specimens showed higher microhardness than that of the ternary alloy with the same Ca and Zn contents (Fig.3).

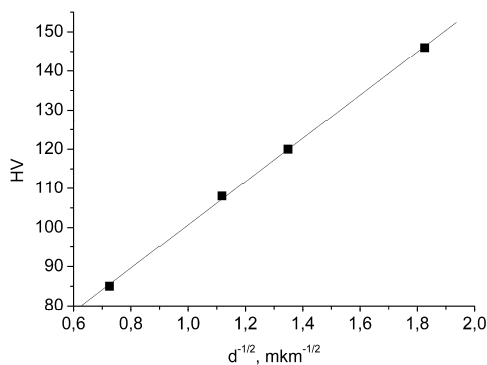


Fig. 4. Hall-Petch plot for as-solidified Mg-Ca-Zn alloys.

Fig. 5 depicts the evolution of magnesium lattice parameter with increasing annealing temperature for the MZC4, MZC5 and MZC6 alloys. The solution of Ca resulted in the expansion and Zn – in the constriction of the Mg lattice [3,7,8,17]. As seen from the figure at the same Ca content the higher Zn content resulted in the smaller lattice size. The reduction of Mg lattice parameters is caused by the decomposition of the supersaturated solid solution. In order to explain the sharp increase of the parameter observed for the MZC4 and MZC5 at 250 and 300 °C correspondently it may be assumed that the stress developed by the structural mismatch between magnesium crystal lattices and the coherent pre-precipitates additionally contracts the magnesium lattice; the growth of the precipitates led to a destruction of the “matrix-precipitate” coherent boundary resulting in a restoration of Mg lattice and observed rise of its parameter; after that, some solid solution decomposition still

continued and, finally, the Mg lattice parameter approached to the value corresponding to the equilibrium solid solution of Mg-0.8 at% Zn [18].

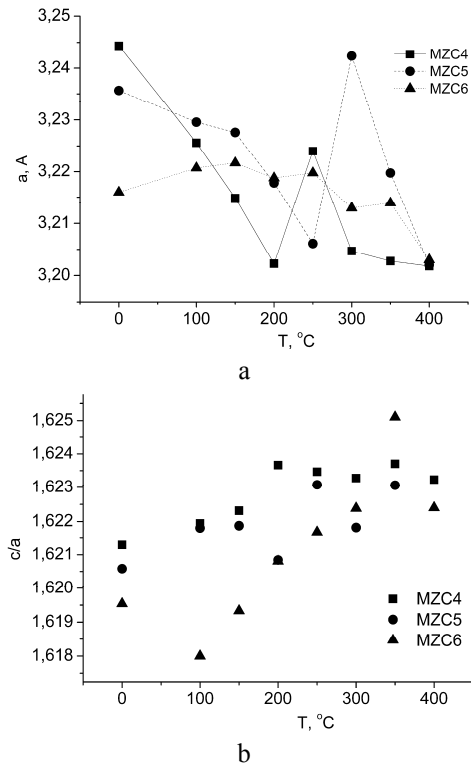


Fig.5. Lattice parameter a (a) and c/a axial ratio (b) of Mg lattice for MZC4, MZC5 and MZC6 alloys vs. annealing temperature.

The high cooling rate (10^7 - 10^8 Kc⁻¹) solidification technique applied to Mg-Ca binary alloys allowed to reduce the c/a ratio to 1.609 at 6.51 at.%Ca dissolved in Mg [17]. Under a cooling rate of 10^5 - 10^6 Kc⁻¹, similar to the one employed in the present work, c/a ratio was observed to be equal to 1.618 [17]. On the contrary, Zn additions maintain the c/a the same as that of pure Mg [1, 17]. In the tested as-solidified alloys, the c/a ratio was less than that for pure Mg, gradually approaching with annealing to magnesium value (Fig. 6(b)). It is noteworthy that the simultaneous additions of Ca and Zn in MZC6 resulted in the significant reduction of the c/a ratio as compared with the alloys containing the same amount of Ca, but less Zn.

Fig. 6 presents the alloys microhardness as a function of the annealing temperature. As the alloys in as-solidified conditions revealed high hardness caused by considerable

microstructural refinement and solid solution hardening the age hardening effect is less pronounced compared to commercial heat-treatable alloys. For example, the microhardness of heat-treated MZC4 is lower than that of as-solidified specimens, obviously for alloys of this compositions the microstructural refinement provided by rapid solidification is more effective than age hardening. However, it can be seen that the age hardening behavior is quite complicated, at least two age hardening phenomena were observed: the first one occurred at 200°C and the second one at 300-350°C. Among the ternary compositions the most noticeable age hardening effect was revealed in MZC5 alloy as it contains optimal alloying elements quantity and (Ca/Zn) ratio allowing to precipitate maximum ternary phase responsible for the age hardening. Quaternary alloys behavior is very similar to that for the ternary one with the same Ca and Zn content. Alloy containing La showed the best hardness in the melt spun state and the most pronounced age hardening effect. Partially, it may be explained by the highest alloying content of the MZCL (Table 1). However, these advantages have been already lost after annealing above 230°C. In respect of high temperature stability the MZCN was chosen as the most promising. There was observed a surprisingly drastic Hv drop for the MZCZ at 300°C, it is supposed to be a result of high coarsening rate of the microstructure refined by Zr [21].

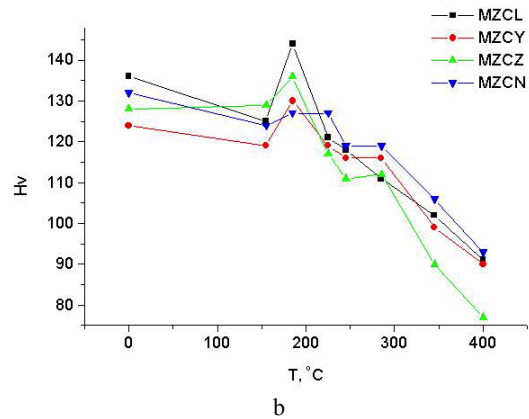
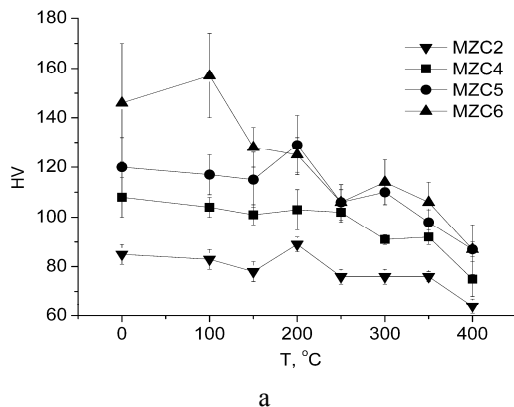


Fig. 6. Vickers microhardness of the ternary (a) and quaternary (b) alloys vs. temperature of the isochronal heat treatment.

To study the hardening phenomena isothermal heat treatment at various temperatures was carried out. Aging curves and corresponding changes of the magnesium matrix lattice parameter (a) are shown in Fig. 7 using an example of the MZCN. It is seen that aging process has a complicated character and develops in at least three stages. The first - low temperature effect was not noticed in isochronal heat treatment aging curves in Fig. 6, but rather clearly may be distinguished in Fig. 7, f at annealing for 30 min at 155°C. It is supposed to be caused by the formation of a large number density of single layer ordered Guiner–Preston (GP) zones. The second hardening phenomenon may be observed in Fig. 6 at 200°C and in Fig. 7, f at 155°C at time of 4 h or in Fig. 7, e at 225°C at time of 1 h. As seen from Fig. 7, b, e, the second hardening effect approximately coincides with the minimum on the lattice parameter dependence (Fig. 7, b, c), similar to that observed on Fig. 5, a. The decrease of the lattice parameter below the value for pure magnesium ($a=3.209\text{\AA}$) is supposed to be caused by a compression of the magnesium lattice due to a stress developed by structural mismatch between crystal lattices of magnesium matrix and precipitates. Formation and growth of coherent pre-precipitates corresponds to hardening effect.

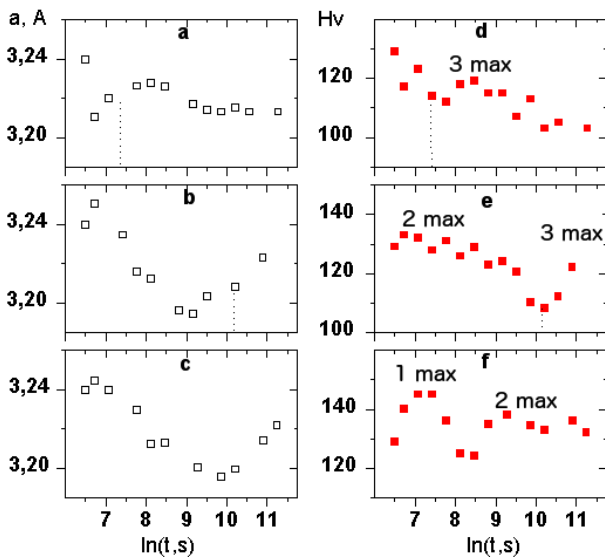


Fig.7. Change of (a-c) *a* lattice parameter of magnesium matrix and (d-f) microhardness with time of isothermal annealing at (a,d) 285°, (b,c) 225° and (e,f) 155°C for MZCN alloy.

In Fig.8 kinetics of this age hardening effect is presented in Arrhenius coordinates, where *T* – an aging temperature and *t_p* - a time to reach a peak hardness.

The apparent activation energy determined by a slope of straight lines is equal to 64 kJ/mol for MZCN and 71 kJ/mol for MZCY respectively. This values are close to that of Mg-Al [10,11], and significantly smaller than apparent activation energy for age hardening of Mg-REM [12,13] and Mg self-diffusion. Such low value may be explained by high concentration of quenched vacancies provided by non-equilibrium solidification.

And the third hardness maximums observed after 1 h at 285°C respectively (Fig. 7,e) is associated with structural rearrangement and equilibrium state formation.

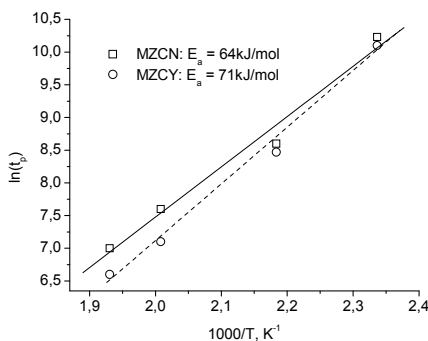


Fig.8. Relationships between natural logarithm of time needed to reach the main peak hardness - *t_p* and

reciprocal aging temperature - $1/T$ for MZCN and MZCY alloys.

Microstructure of the as-solidified and heat treated samples are presented in Figure 9 using an example of the MZCN. Melt spun MZCN ribbons had a fine structure with a cell size of 0.2-0.5 mkm (Fig.10,a) it is two times smaller than that of the ternary Mg-Ca-Zn. Very fine lamellar precipitates, mostly Mg_2Ca (as revealed by XRD) located along the cell peripheries. After heat treatment corresponding to the second hardening phenomenon (Fig.7,e,f) the microstructure changed drastically (Fig.9,b): the cellular structure disappeared and very fine and uniformly distributed precipitates emerged. At further annealing homogeneously distributed spherical precipitates of size about 50-200 nm appeared (Fig.9,c). Grain boundaries became discerned and grain size increased up to 1–2 mkm. This microstructure corresponds to a minimum of *Hv* (Fig.7,e). I

Conclusions

Depending on the composition, the studied alloys solidified as a single phase - Mg-based solid solution, two phase mixtures - Mg solid solution and Mg_2Ca or $\text{Mg}_6\text{Ca}_2\text{Zn}_3$ or three phase mixture - Mg solid solution, Mg_2Ca and $\text{Mg}_6\text{Ca}_2\text{Zn}_3$. No phases containing La, Y, Nd, Zr have been found.

As-solidified ternary alloys exhibited hardening according to the following: $\text{HV} = 50 + 18C_{\text{Ca}} + 8C_{\text{Zn}}$, where C_{Ca} and C_{Zn} are Ca and Zn content correspondently. The higher Ca impact is explained by its stronger refinement effect. Microalloying additions of La, Y, Nd, Zr resulted in an additional refinement and, correspondingly, strengthening.

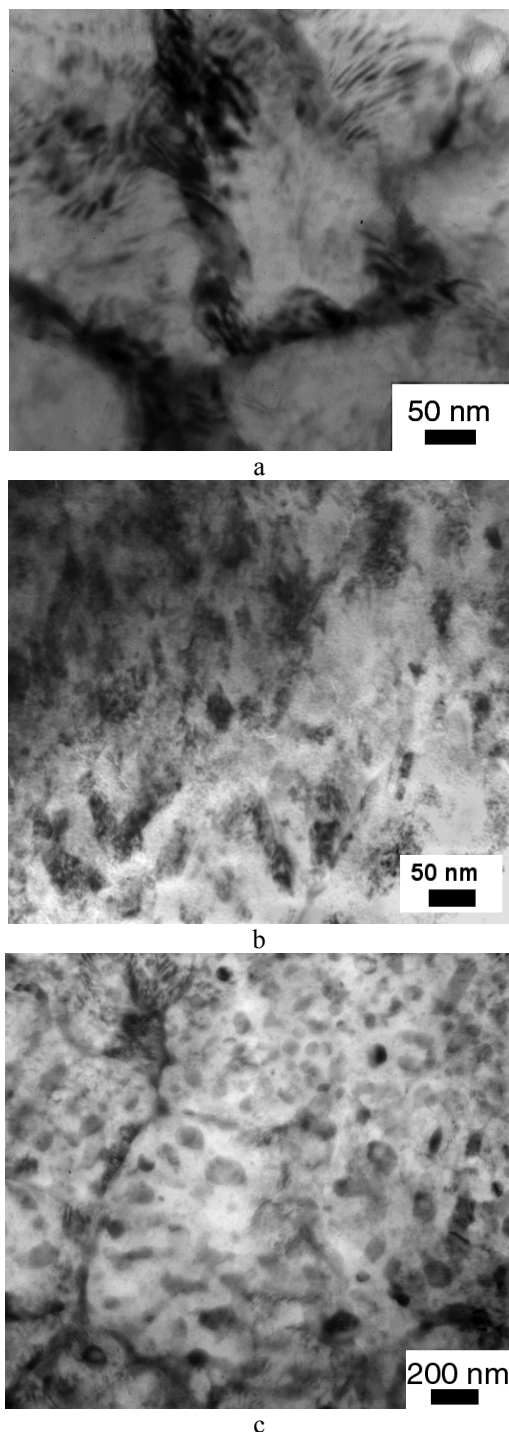


Fig.9. Microstructures of MZCN alloy in (a) melt spun and (b-c) annealed conditions: (b) at T=185°C for 1h and (c) at T=185°C for 8h.

The complicated age hardening behavior was observed. The most pronounced age hardening phenomenon occurred after 1 hour heating at 200-250°C. Among the ternary compositions the most noticeable age hardening effect was revealed in Mg-3at.%Ca-2at.%Zn alloy as it contains optimal alloying elements quantity and (Ca/Zn) ratio allowing to

precipitate maximum phase responsible for the age hardening. The alloy containing La addition exhibited the highest microhardness in as-solidified state and the most pronounced age hardening response. In respect of high temperature stability Nd addition appeared to be the most effective.

References:

- [1] Hehmann F. , H. Jones, in: T.S. Srivatsan, T.S. Sudarshan (Eds.), *Rapid Solidification Technology: An Engineering Guide*. Technomic Publishing Inc., 1993, pp. 441–471
- [2] J.Gay, G.C.Ma, Z.Liu, H.F.Zhang, A.M.Wang, Z.Q.Hu, Influence of Rapid Solidification on The Mechanical Properties Of Mg-Zn-Ce-Ag Magnesium Alloy, *Mater. Sci. Eng. A* 456 (2007) 364-367.
- [3] D. Themines, W. Riehemann, W. Henning and B.L. Mordike, in: *Mat. Res. Soc. Symp. Proc. Material Research Society*, 58 (1986) 275.
- [4] W.P. Yanga, X.F. Guo, Z.X. Lu, Crystal structure of the ternary Mg-Zn-Ce phase in rapidly solidified Mg-6Zn-1Y-1Ce alloy, *Journal of Alloys and Compounds*, 521 (2012) 1–3.
- [5] You B. S., Park W. W. and I. S. Chung, The Effect of Calcium Additions On The Oxidation Behavior In Magnesium Alloys, *Scripta Mater.*, 42 (2000) 1089-1094.
- [6] C. D. Yim, Y. M. Kim, B. S. You, Effect of Ca Addition on the Corrosion Resistance of Gravity Cast AZ31 Magnesium Alloy, *Materials Transactions*, Vol. 48, No. 5 (2007) 1023-1028.
- [7] K.Hantzsche, J. Bohlen,a, J. Wendt, K.U. Kainer, S.B. Yi, D. Letzig, Effect of rare earth additions on microstructure and texture development of magnesium alloy sheets, *Scripta Materialia* 63 (2010) 725–730
- [8] K. Hono, C.L. Mendis, T.T. Sasaki, K. Oh-ishi, Towards the development of heat-treatable high-strength wrought Mg alloys, *Scripta Materialia* 63 (2010) 710–715
- [9] T. Miyazaki, J. Kaneko, M. Sugamata, Structures And Properties Of Rapidly Solidified Mg-Ca Based Alloys, *Mater. Sci. Eng. A*181/A182 (1994) 1410-1414.
- [10]L. L. Rokhlin, T.V. Dobatkina, I. G. Korol’kova, Mg-Ca and Mg-Nd Alloys Prepared by Rapid Solidification, *Metally*, 2 (1994) 152-158.
- [11]B. Langelier, S. Esmaili, The Effect of Zn Additions on Precipitation Hardening of Mg-Ca Alloys, *Proc. Symp. Magnesium Technology*, TMS (2010).
- [12]P.Vostrý, I.Stulikova, B. Smola, Structure and Stability of Microcrystalline Mg-Ca Alloy, *Mater. Sci. Eng., A* 137 (1991) 87-92.

- [13] T. Larionova, W.-W. Park, B.-S. You, A Ternary Phase Observed in Rapidly Solidified Mg-Ca-Zn Alloys, *Scripta Mater.*, 45 (2001) 7-12.
- [14] Y.N. Zhang, G.J. Rocher, B. Briccoli, D. Kevorkov, X.B. Liu, Z. Altounian, M. Medraj, Crystallization characteristics of the Mg-rich metallic glasses in the Ca-Mg-Zn system, *Journal of Alloys and Compounds*, 552 (2013) 88-97.
- [15] N. Zhang, D. Kevorkov, X. D. Liu, F. Bridierc, P. Chartrand, M. Medraj, Homogeneity range and crystal structure of the $\text{Ca}_2\text{Mg}_5\text{Zn}_{13}$ compound, *Journal of Alloys and Compounds*, 523 (2012) 75-82.
- [16] F. Knoop, B. Mordike, P. Lukas, Proc. of the third international magnesium conference (1997), pp. 465.
- [17] C. Shaw, H. Jones, The Contributions of Different Alloying Additions To Hardening In Rapidly Solidified Magnesium Alloys, *Mater.Sci.Eng., A* 226-228 (1997) 856-860.
- [18] J.A.Juarez-Islas, Rapid solidification of Mg-Al-Zn-Si alloys *Mater.Sci.Eng., A*134 (1991) 1193-1196.
- [19] F. Hehmann, F. Sommer, B. Predel, Extension of Solid Solubility In Magnesium By Rapid Solidification, *Mater. Sci. Eng.* A125, (1990) 249-265.
- [20] B.L.Mordike, W.Riehemann, Mechanical Properties And Thermal Stability of Rapidly Solidified Magnesium Alloys, *Key Engineering Materials*, 97-98 (1994) 13-28.
- [21] M. Bamberger, G. Levi, and J. Vander Sande, "Precipitation Hardening in Mg-Ca-Zn Alloys," *Metallurgical and Materials Transactions A*, 37 (2006), p. 481-487.

Contact Author Email Address

Mail to: larionova@hotmail.com

Copyright Statement

The authors confirm that they, and/or their company or organization, hold copyright on all of the original material included in this paper. The authors also confirm that they have obtained permission, from the copyright holder of any third party material included in this paper, to publish it as part of their paper. The authors confirm that they give permission, or have obtained permission from the copyright holder of this paper, for the publication and distribution of this paper as part of the ICAS 2014 proceedings or as individual off-prints from the proceedings.